Inorg. Chem. **2006**, *45*, 10882−10894

Phenylazo-pyridine and Phenylazo-pyrazole Chlorido Ruthenium(II) Arene Complexes: Arene Loss, Aquation, and Cancer Cell Cytotoxicity

Sarah J. Dougan, Michael Melchart, Abraha Habtemariam, Simon Parsons, and Peter J. Sadler*

School of Chemistry, University of Edinburgh, West Mains Road, Edinburgh EH9 3JJ, U.K.

Received August 3, 2006

Ru(II) η^6-arene complexes containing *p*-cymene (*p*-cym), tetrahydronaphthalene (thn), benzene (bz), or biphenyl (bip), as the arene, phenylazopyridine derivatives ($C_5H_4NN{:}NC_6H_5R$; R = H (azpy), OH (azpy-OH), NMe_2 (azpy-NMe_2)) or a phenylazopyrazole derivative ($NHC_3H_2NN{:}NC_6H_5NMe_2$ (azpyz-NMe_2)) as N,N-chelating ligands and chloride as a ligand have been synthesized (**1**–**16**). The complexes are all intensely colored due to metal-to-ligand charge-transfer Ru $4d^6$–π^* and intraligand $\pi \rightarrow \pi^*$ transitions (ϵ = 5000–63 700 M^{-1} cm^{-1}) occurring in the visible region. In the crystal structures of [(η^6-*p*-cym)Ru(azpy)Cl]PF_6 (**1**), [(η^6-*p*-cym)Ru(azpy-NMe_2)Cl]PF_6 (**5**), and [(η^6-bip)Ru(azpy)Cl]PF_6 (**4**), the relatively long Ru–N(azo) and Ru–(arene-centroid) distances suggest that phenylazopyridine and arene ligands can act as competitive π-acceptors toward Ru(II) $4d^6$ electrons. The pK_a* values of the pyridine nitrogens of the ligands are low (azpy 2.47, azpy-OH 3.06 and azpy-NMe_2 4.60), suggesting that they are weak σ-donors. This, together with their π-acceptor behavior, serves to increase the positive charge on ruthenium, and together with the π-acidic η^6-arene, partially accounts for the slow decomposition of the complexes via hydrolysis and/or arene loss ($t_{1/2}$ = 9–21 h for azopyridine complexes, 310 K). The pK_a* of the coordinated water in [(η^6-*p*-cym)Ru(azpyz-NMe_2)OH_2]$^{2+}$ (**13A**) is 4.60, consistent with the increased acidity of the ruthenium center upon coordination to the azo ligand. None of the azpy complexes were cytotoxic toward A2780 human ovarian or A549 human lung cancer cells, but several of the azpy-NMe_2, azpy-OH, and azpyz-NMe_2 complexes were active (IC_{50} values 18–88 μM).

Introduction

Ruthenium complexes have potential as anticancer drugs.[1] We have previously reported that ruthenium(II) arene complexes of the type [(η^6-arene)Ru^{II}(XY)Z]$^+$, where XY is a chelating diamine and Z is a leaving group, exhibit cytotoxicity against several cancer cell lines including cisplatin-resistant cells.[2,3] Increased hydrophobicity of the arene increases cytotoxicity and complexes containing chelating diamines were more active than complexes containing only monodentate ligands. It has been proposed that hydrolysis of the reactive ruthenium−chloride bond may activate the complex for DNA binding[4] and that distortions of DNA may contribute to the mechanism of action.[5] In these types of complexes, ruthenium is stabilized in the +2 oxidation state by the π-acidic η^6-arene and in the case of ethylenediamine (en), the chelating diamine N ligands are σ-donors. In this paper we investigate how changes in the nature of the bonding by the chelating ligand affect the cytotoxic properties of Ru(II) arene complexes.

Azo ligands, such as 2-phenylazopyridine (azpy), which contain the −N=N−C=N− linkage have unusual properties.[6] The pyridine ring is an intermediate π-acceptor, and its nitrogen is a weak σ-donor. The azo group has low σ-donor ability to the metal, but possesses enhanced π-accepting ability through the azo π^* orbital. Consequently, chelating ligands of this type are able to stabilize metals in their lower oxidation states. Several ruthenium(II) compounds containing such ligands have been reported previ-

* To whom correspondence should be addressed. E-mail: p.j.sadler@ed.ac.uk.

(1) Clarke, M. J. *Coord. Chem. Rev.* **2003**, *236*, 209−233.
(2) Morris, R. E.; Aird, R. E.; del Socorro Murdoch, P.; Chen, H,; Cummings, J.; Hughes, N. D, Parsons, S.; Parkin, A.; Boyd, G.; Jodrell, D. I.; Sadler, P. J. *J. Med. Chem.* **2001**, *44*, 3616−3621.
(3) Aird, R. E.; Cummings, J.; Ritchie, A. A.; Muir, M.; Morris, R. E.; Chen, H.; Sadler, P. J.; Jodrell, D. I. *Br. J. Cancer*. **2002**, *86*, 1652−1657.
(4) Chen, H.; Parkinson, J. A.; Morris, R. E.; Sadler, P. J. *J. Am. Chem. Soc.* **2003**, *125*, 173−186.
(5) Novakova, O.; Chen, H.; Vrana, O.; Rodger, A.; Sadler, P. J.; Brabec, V. *Biochemistry* **2003**, *42*, 11544−11554.
(6) Velders, A. H.; van der Schilden, K.; Hotze, A. C. G.; Reedijk, J.; Kooijman, H.; Spek, A. L. *J. Chem. Soc., Dalton Trans.* **2004**, 448−455.

10.1021/ic061460h CCC: $33.50
Published on Web 12/07/2006

ously.[7,8] For example, the cytotoxic properties of isomers and derivatives of $[Ru(azpy)_2Cl_2]$ have been investigated in several cancer cell lines.[9−12] In particular, α-$[Ru(azpy)_2Cl_2]$ (α = trans pyridines, cis azo nitrogens, and cis chlorides) was found to be highly active against a broad range of cancer cell lines, with cytotoxicities comparable to cisplatin and 5-fluorouracil and superior activity in faster-growing cell lines.

We report here the synthesis, characterization, and cytotoxicity of a series of novel ruthenium(II) complexes containing both an η^6-coordinated arene and a chelated 2-phenylazopyridine or phenylazopyrazole derivative. We have investigated how variations in the arene and the chelating ligand influence the electronic, structural, and cytotoxic properties of such complexes and studied their aqueous solution chemistry. The nature of the bonding in these complexes is also discussed and is related to the experimental data.

Experimental Section

Materials. The preparations of the starting materials $[(\eta^6\text{-arene})RuCl_2]_2$ (arene = *p*-cymene, tetrahydronaphthalene, benzene, biphenyl) were based on literature reports.[13,14] 4-(2-Pyridylazo)-*N*,*N*-dimethylaniline (azpy-NMe_2), aniline, $NaNO_2$, 2-cyanoethylhydrazine, *N*,*N*-dimethylaniline, *o*-phosphoric acid, benzoquinone, 2-hydrazinopyridine, and $NOHSO_4$ were purchased from Sigma-Aldrich. Ethanol and methanol were dried over Mg/I_2 or anhydrous quality was used (Sigma-Aldrich). The ruthenium ICP-OES standard (1000 ppm) was purchased from Sigma-Aldrich. All other reagents used were obtained from commercial suppliers and used as received.

Synthesis of Chelating Azo Ligands. Syntheses of azpy, azpyz-NMe_2, and azpy-OH can be found in the Supporting Information.

Synthesis of Ruthenium Complexes. All compounds were synthesized using a similar procedure. Typically, the ligand (2 mol equiv) dissolved in methanol was added dropwise to a solution of the ruthenium dimer $[(\eta^6\text{-arene})RuCl_2]_2$ (1 mol equiv) in methanol. The solution immediately changed color and was stirred at ambient temperature, the volume of solvent was reduced, NH_4PF_6 (10 mol equiv) was added, and the precipitate, obtained after storage in a freezer overnight at ca. 255 K, was filtered off, washed with ether, and dried overnight in vacuo. Details of the amounts of reactants, volumes of methanol, color changes, stirring times, and nature of the product are described below for the individual reactions, as well as any variations in the synthetic procedure.

$[(\eta^6\text{-}p\text{-cym})Ru(azpy)Cl]PF_6$ (1). $[(\eta^6\text{-}p\text{-cym})RuCl_2]_2$ (258 mg, 0.42 mmol) in 25 mL of methanol and azpy (156 mg, 0.85 mmol) in 10 mL of methanol; solution turned from brown to deep red; stirred for 1 h; black powder. Yield: 408 mg (80.9%) (Found: C, 42.09; H, 4.02; N, 7.03. Calcd for $RuC_{21}H_{23}N_3ClPF_6$: C, 42.11; H, 3.87; N, 7.02). ^{1}H NMR ($CDCl_3$): δ 9.45 (1H, d), 8.58 (1H, d), 8.27 (1H, t), 8.09 (2H, m), 7.90 (1H, t), 7.77 (1H, t), 7.67 (2H, t), 6.24 (1H, d), 5.90 (1H, d) 5.77 (2H, dd), 2.53, (1H, m), 2.23 (3H, s), 1.10 (3H, d), 1.02 (3H, d).

$[(\eta^6\text{-thn})Ru(azpy)Cl]PF_6$ (2). $[(\eta^6\text{-thn})RuCl_2]_2$ (100 mg, 0.16 mmol) in 20 mL of methanol and azpy (60 mg, 0.33 mmol) in 15 mL of methanol; solution turned from orange to dark brown; stirred for 1 h; black shiny powder. Yield: 166 mg (86.7%) (Found: C, 41.35; H, 3.67; N, 6.98. Calcd for $RuC_{21}H_{21}N_3ClPF_6$: C, 42.26; H, 3.55; N, 7.04). ^{1}H NMR ($CDCl_3$): δ 9.14 (1H, d), 8.63 (1H, d), 8.27 (1H, t), 8.07 (2H, m), 7.83 (1H, t), 7.72 (1H, t), 7.66 (2H, t), 6.01 (1H, d), 5.84 (1H, t), 5.56 (1H, d), 5.34 (1H, t), 2.92−2.64 (4H, m), 2.03−1.76 (4H, m).

$[(\eta^6\text{-bz})Ru(azpy)Cl]PF_6$ (3). $[(\eta^6\text{-bz})RuCl_2]_2$ (51 mg, 0.10 mmol) in 25 mL of methanol and azpy (38 mg, 0.21 mmol) in 15 mL of methanol; solution turned from light to dark brown; stirred for 1 h; dark brown powder. Yield: 81.6 mg (73.7%) (Found: C, 37.82; H, 2.73; N, 7.63. Calcd for $RuC_{17}H_{15}N_3ClPF_6$: C, 37.62; H, 2.79; N, 7.74). ^{1}H NMR ($(CD_3)_2SO$): δ 9.80 (1H, d), 8.90 (1H, d), 8.61 (1H, t), 8.31 (2H, m), 8.03 (1H, t), 7.82−7.79 (3H, m), 6.43 (6H, s).

$[(\eta^6\text{-bip})Ru(azpy)Cl]PF_6$ (4). $[(\eta^6\text{-bip})RuCl_2]_2$ (102 mg, 0.16 mmol) in 40 mL of methanol and 10 mL of water refluxed under argon for 2 h; hot-filtered to remove black residue then azpy (63 mg, 0.34 mmol) in 20 mL of methanol added; solution turned from orange to deep red; stirred and left to cool to ambient temperature for 1 h; left in the fridge overnight; light brown powder. Yield: 130 mg (68.3%) (Found: C, 44.11; H, 2.92; N, 6.85. Calcd for $RuC_{23}H_{19}N_3ClPF_6$: C, 44.64; H, 3.09; N, 6.79). ^{1}H NMR ($(CD_3)_2CO$): δ 9.55 (1H, d), 8.88 (1H, d), 8.57 (1H, t), 8.10 (2H, d), 7.95 (1H, t), 7.80 (1H, t), 7.76 (2H, d), 7.67−7.59 (3H, m), 7.53 (2H, t), 6.82−6.77 (2H, m), 6.69 (2H, d of t), 6.45 (1H, t).

$[(\eta^6\text{-}p\text{-cym})Ru(azpy\text{-}NMe_2)Cl]PF_6$ (5). $[(\eta^6\text{-}p\text{-cym})RuCl_2]_2$ (256 mg, 0.42 mmol) in 25 mL of methanol and azpy-NMe_2 (185 mg, 0.82 mmol) in 10 mL of methanol; solution turned from brown to dark blue; stirred for 1 h; black microcrystalline solid. Yield: 480 mg (91.8%) (Found: C, 43.19; H, 4.52; N, 8.62. Calcd for $RuC_{23}H_{28}N_4ClPF_6$: C, 43.03; H, 4.40; N, 8.73). ^{1}H NMR ($CDCl_3$): δ 9.22 (1H, d), 8.2−8.15 (3H, m), 8.07 (1H, t), 7.62 (1H, t), 6.82 (2H, d), 6.03 (1H, d), 5.85 (1H, d), 5.76 (2H, dd), 3.31 (6H, s), 2.48 (1H, m), 2.27 (3H, s), 1.43 (3H, d), 0.61 (3H, d).

$[(\eta^6\text{-thn})Ru(azpy\text{-}NMe_2)Cl]PF_6$ (6). $[(\eta^6\text{-thn})RuCl_2]_2$ (105 mg, 0.17 mmol) in 25 mL of methanol and azpy-NMe_2 (75 mg, 0.33 mmol) in 15 mL of methanol; solution immediately turned from orange to dark blue; stirred for 1.5 h; green powder. Yield: 188 mg (90.6%) (Found: C, 42.40; H, 4.22; N, 8.81. Calcd for $RuC_{23}H_{26}N_3ClPF_6$: C, 43.17; H, 4.09; N, 8.75). ^{1}H NMR ($CDCl_3$): δ 9.03 (1H, d), 8.21 (3H, m), 8.09 (1H, t), 7.61 (1H, t), 6.83 (2H, d), 5.89 (1H, t), 5.83 (1H, t), 5.79 (2H, m), 3.31 (6H, s), 2.74−2.39 (4H, m), 1.79−1.58 (4H, m).

$[(\eta^6\text{-bz})Ru(azpy\text{-}NMe_2)Cl]PF_6$ (7). $[(\eta^6\text{-bz})RuCl_2]_2$ (51 mg, 0.10 mmol) and azpy-NMe_2 (46 mg, 0.20 mmol), solution immediately turned from orange to dark blue-purple. Solution was stirred for 1 h. A dark brown powder was obtained. Yield: 86 mg (73.4%) (Found: C, 39.05; H, 3.29; N, 9.48. Calcd for $RuC_{19}H_{20}N_4ClPF_6$: C, 38.95; H, 3.44; N, 9.56). ^{1}H NMR ($(CD_3)_2CO$): δ 9.56 (1H, d), 8.43−8.33 (4H, m), 7.72 (1H, t), 7.05 (2H, d), 6.35 (6H, s), 3.39 (6H, s).

$[(\eta^6\text{-bip})Ru(azpy\text{-}NMe_2)Cl]PF_6$ (8). $[(\eta^6\text{-bip})RuCl_2]_2$ (105 mg, 0.16 mmol) in 40 mL of methanol and 10 mL of water refluxed under argon for 2 h then azpy-NMe_2 (78 mg, 0.35 mmol) in 20

(7) Lahiri, G. K.; Bhattacharya, S.; Goswami, S., Chakavorty, A. *J. Chem. Soc., Dalton Trans.* **1990**, 561−565.
(8) Krause, R. A.; Krause, K. *Inorg. Chem.* **1982**, *21*, 1714−1720.
(9) Velders, A. H.; Kooijman, H.; Spek, A. L.; Haasnoot, J. G.; De Vos, D.; Reedijk, J. *Inorg. Chem.* **2000**, *39*, 2966−2967.
(10) Hotze, A. C. G.; Bacac, M.; Velders, A. H.; Jansen, B. A. J.; Kooijman, H.; Spek, A. L.; Haasnoot, J. G.; Reedijk, J. *J. Med. Chem.* **2003**, *46*, 1743−1750.
(11) Hotze, A. C. G.; Caspers, S. E.; de Vos, D.; Kooijman, H.; Spek, A. L.; Flamigni, A.; Bacac, M.; Sava, G.; Haasnoot, J. G.; Reedijk, J. *J. Biol. Inorg. Chem.* **2004**, *9*, 354−364.
(12) Hotze, A. C. G.; van der Geer, E. P. L.; Kooijman, H.; Spek, A. L.; Haasnoot, J. G.; Reedijk, J. *Eur. J. Inorg. Chem.* **2005**, 2648−2657.
(13) Bennett, M. A.; Smith, A. K. *J. Chem. Soc., Dalton Trans.* **1974**, 233−241.
(14) Zelonka, R. A.; Baird, M. C. *J. Organomet. Chem.* **1972**, *35*, C43−C46.

mL of methanol added; solution turned from brown to very dark blue; mixture hot-filtered and left to cool to ambient temperature while stirring for 30 min; left in the fridge overnight; black crystalline powder. Yield: 130 mg (61.1%) (Found: C, 45.31; H, 3.56; N, 8.44. Calcd for $RuC_{25}H_{24}N_4ClPF_6$: C, 45.36; H, 3.65; N, 8.46). ^{1}H NMR ($(CD_3)_2CO$): δ 9.25 (1H, d), 8.36 (1H, d), 8.29 (1H, t), 8.22 (2H, d), 7.75−7.71 (2H, m), 7.60−755 (2H, m), 7.54−7.48 (2H, t), 6.91 (2H, d), 6.75 (1H, d), 6.65 (1H, d), 6.57 (2H, d of d), 6.38 (1H, t), 3.36 (6H, s).

[(η^6-*p*-cym)Ru(azpy-OH)Cl]PF$_6$ (9). [(η^6-*p*-cym)$RuCl_2]_2$ (40 mg, 0.05 mmol) in 10 mL of methanol and azpy-OH (21 mg, 0.11 mmol) in 10 mL of methanol; solution turned from brown to deep brown-red with a yellow tinge; stirred for 3 h; black powder. Yield: 50 mg (84.7%). ^{1}H NMR ($(CD_3)_2SO$): δ 9.49 (d, 1H), 8.55 (d, 1H), 8.37 (t, 1H), 8.12 (d, 2H), 7.80 (t, 1H), 6.99 (d, 2H), 6.40 (d, 1H), 6.16 (t, 2H), 6.06 (d, 1H), 2.37 (septet, 1H), 2.23 (s, 3H), 0.88 (dd, 6H). ESI-MS: calcd for $RuC_{21}H_{23}N_3O^+$ [M^+] *m*/*z* 470.1, found 469.9.

[(η^6-thn)Ru(azpy-OH)Cl]PF$_6$ (10). [(η^6-thn)$RuCl_2]_2$ (30 mg, 0.05 mmol) in 20 mL of methanol and azpy-OH (21 mg, 0.11 mmol) in 15 mL of methanol; solution turned from orange to deep brown-red with a yellow tinge; stirred for 2 h; black powder. Yield: 45 mg (73.4%) (Found: C, 40.79; H, 3.19; N, 6.78. Calcd for $RuC_{21}H_{21}N_3ClOPF_6$: C, 41.15; H, 3.45; N, 6.86). ^{1}H NMR ($(CD_3)_2SO$) δ 9.49 (d, 1H), 8.71 (d, 1H), 8.45 (t, 1H), 8.16 (d, 2H), 7.94 (t, 1H), 7.08 (d, 2H), 6.39 (d, 1H), 6.25 (t, 1H), 6.095 (t, 1H), 6.06 (d, 1H), 2.71−2.62 (m, 1H), 2.62−2.5 (m, 1H), 2.34−2.25 (m, 1H), 2.15−2.06 (m, 1H), 1.62−1.49 (m, 2H), 1.33−1.11 (m, 2H).

[(η^6-bz)Ru(azpy-OH)Cl]PF$_6$ (11). [(η^6-bz)$RuCl_2]_2$ (25 mg, 0.05 mmol) in 10 mL of methanol and azpy-OH (20 mg, 0.10 mmol) in 5 mL of methanol; solution turned from brown to deep brown-red with a yellow tinge; stirred for 4 h; black solid. Yield: 35 mg (62.6%) (Found: C, 36.65; H, 2.50; N, 7.60. Calcd for $RuC_{17}H_{15}N_3ClOPF_6$: C, 36.54; H, 2.71; N, 7.52). ^{1}H NMR ($(CD_3)_2SO$): δ 9.66 (d, 1H), 8.71 (d, 1H), 8.44 (t, 1H), 8.19 (d, 2H), 7.89 (t, 1H), 7.05 (d, 2H), 6.29 (s, 6H).

[(η^6-bip)Ru(azpy-OH)Cl]PF$_6$ (12). [(η^6-bip)$RuCl_2]_2$ (30 mg, 0.05 mmol) in 40 mL of methanol and 10 mL of water refluxed under argon for 2 h; azpy-OH (20 mg, 0.10 mmol) in 15 mL of methanol added; solution turned from brown to deep brown-red with a yellow tinge; hot-filtered and left to cool to ambient temperature while stirring for 30 min; left in fridge overnight; brown microcrystalline solid. Yield: 45 mg (46.0%) ^{1}H NMR ($(CD_3)_2SO$): δ 9.41 (d, 1H), 8.63 (d, 1H), 8.36 (t, 1H), 7.99 (d, 2H), 7.74 (t, 1H), 7.63 (d, 2H), 7.54 (t, 1H), 7.46 (t, 2H), 6.90 (d, 2H), 6.79 (d, 1H), 6.78 (d, 1H), 6.57 (t, 1H), 6.49 (t, 1H), 6.30 (t, 1H). ESI MS: Calcd for $RuC_{23}H_{19}N_3O^+$ [M^+] *m*/*z* 491.0, found 489.75.

[(η^6-*p*-cym)Ru(azpyz-NMe$_2$)Cl]PF$_6$ (13). [(η^6-*p*-cym)$RuCl_2]_2$ (103 mg, 0.17 mmol) in 30 mL of methanol and azpyz-NMe_2 (69 mg, 0.32 mmol) in 10 mL of methanol; solution turned from brown to deep purple; stirred for 1 h; black powder. Yield: 126 mg (62.4%) (Found: C, 40.35; H, 4.06; N, 10.56. Calcd for $RuC_{21}H_{27}N_5ClPF_6$: C, 39.98; H, 4.31; N, 11.10). ^{1}H NMR ($CDCl_3$): δ 8.02 (d, 2H), 7.95 (d, 1H), 7.07 (d, 1H), 6.77 (d, 2H), 6.34 (dd, 2H), 5.68 (dd, 2H), 3.22 (s, 6H), 2.4−2.33 (m, 4H), 0.92 (dd, 6H).

[(η^6-thn)Ru(azpyz-NMe$_2$)Cl]PF$_6$ (14). [(η^6-thn)$RuCl_2]_2$ (30 mg, 0.05 mmol) in 10 mL of methanol and azpyz-NMe_2 (21 mg, 0.10 mmol) in 10 mL of methanol; solution turned from orange to deep purple; stirred for 1 h; black powder. Yield: 46 mg (74.6%). ^{1}H NMR ($CDCl_3$): δ 8.15 (m, 3H), 7.21 (d, 1H), 6.93 (d, 2H), 6.35 (d, 1H), 6.0−5.8 (m, 3H), 3.24 (s, 6H), 3.0−1.5 (m, 8H). ESI MS: calcd for $RuC_{21}H_{25}N_5Cl^+$ [M^+] *m*/*z* 484.1, found 483.9.

[(η^6-bz)Ru(azpyz-NMe$_2$)Cl]PF$_6$ (15). [(η^6-bz)$RuCl_2]_2$ (50 mg, 0.10 mmol) in 30 mL of methanol and azpyz-NMe_2 (42 mg, 0.20 mmol) in 15 mL of methanol; solution turned from brown to deep purple; stirred for 2 h; black powder. Yield: 92 mg (80.0%) (Found: C, 34.89; H, 2.68; N, 12.18. Calcd for $RuC_{17}H_{19}N_5ClPF_6$: C, 35.52; H, 3.33; N, 12.18). ^{1}H NMR ($(CD_3)_2CO$): δ 8.31 (d, 1H), 8.21 (d, 2H), 7.31 (d, 1H), 6.96 (d, 2H), 6.29 (s, 6H), 3.28 (s, 6H).

[(η^6-bip)Ru(azpyz-NMe$_2$)Cl]PF$_6$ (16). [(η^6-bip)$RuCl_2]_2$ (100 mg, 0.17 mmol) in 40 mL of methanol and 10 mL of water refluxed under argon for 2 h and hot-filtered to remove a small amount of black residue; azpyz-NMe_2 (74 mg, 0.35 mmol) in 10 mL of methanol; solution turned from orange-brown to deep purple; stirred and left to cool to ambient temperature for 3 h; left in the fridge overnight; black powder. Yield: 153 mg (67.2%) (Found: C, 42.97; H, 3.50; N, 11.70. Calcd for $RuC_{23}H_{23}N_5ClPF_6$: C, 42.44; H, 3.56; N, 10.76). ^{1}H NMR ($(CD_3)_2CO$): δ 8.21 (d, 1H), 8.04 (d, 2H), 7.71−7.34 (m, 5H), 7.29 (d, 1H), 6.81 (d, 2H), 6.71 (d, 1H), 6.66−6.55 (m, 2H), 6.52 (t, 1H), 6.31 (t, 1H), 3.25 (s, 6H).

Instrumentation. X-ray Crystallography. All diffraction data were collected on a Bruker Smart Apex CCD diffractometer operating at 150 K using Mo Kα radiation (λ = 0.71073Å). The crystal structure of **1** was solved using direct methods (SHELXS)[15] and was refined against F^2 using SHELXL.[16] The crystal structures of **4** and **5** were solved using Patterson methods (DIRDIF)[17] and were refined against F^2 using SHELXL or CRYSTALS.[18] In all cases the hydrogen atoms were placed in calculated positions and non-hydrogen atoms were refined with anisotropic displacement parameters. Crystals of **4** formed in clumplike aggregates. The diffraction pattern from the sample selected for data collection was indexed on the basis of two orientation matrices. The relationship between these matrices (the 'twin law') could be expressed with the matrix

$$\begin{pmatrix} -0.955 & -0.011 & -0.111 \\ -0.428 & -0.482 & 0.574 \\ -0.404 & 1.282 & 0.456 \end{pmatrix}$$

The data set used for structure elucidation was taken from the more strongly diffracting of the two domains. The crystal structures of **1**, **4**, and **5** have been deposited in the Cambridge Crystallographic Data Centre under the accession numbers CCDC 616620, 616621, and 616622, respectively.

Crystal Data for Complex 1. Crystals suitable for X-ray diffraction were obtained by diffusion of diethyl ether into an acetone solution at ambient temperature. The sample was dark green block of dimensions 0.23 × 0.22 × 0.18 mm^3: triclinic, space group $P\bar{1}$; a = 9.1789(10) Å, b = 9.7628 (11) Å, c = 13.0987(14) Å; α = 84.688(1)°, β = 72.951(2)°, γ = 89.795(1)°; V = 1117.1(2) Å^3; Z = 1; D_{calc} = 1.781 Mg m^{-3}; μ = 0.958 mm^{-1}; F(000) = 600. The final conventional R factor [R1, based on $|F|$ and 3651 data with $F > 4\sigma(F)$] was 0.0350, and weighted wR2 (based on F^2 and all 5695 unique data from θ = 1.63−25.0°) was 0.0872. The final ΔF synthesis extremes were +0.84 and −0.54 e Å^{-3}.

(15) Sheldrick, G. M. *SHELXS*; University of Göttingen: Göttingen, Germany, 1997.
(16) Sheldrick, G. M. *SHELXL*; University of Göttingen: Göttingen, Germany, 1997
(17) Beurskens, P. T.; Beurskens, G.; Gelder, R. D.; Garcia-Granda, S.; Gould, R. O.; Israel, R.; Smits, J. M. M. Crystallography Laboratory; University of Nijmegen: Nijmegen, The Netherlands 1999.
(18) Betteridge, P. W.; Carruthers, J. R.; Cooper, R. I.; Prout, K.; Watkin, D. J. *J. Appl. Crystallogr.* **2003**, *36*, 1487.

Crystal Data for Complex 4. Crystals suitable for X-ray diffraction were obtained by slow evaporation of an acetone/toluene solution at ambient temperature. The sample was a red lath of dimensions 0.66 × 0.43 × 0.20 mm^3: orthorhombic, space group *Pbca*; $a = 10.0146(4)$ Å, $b = 17.6860(7)$ Å, $c = 25.9129(10)$ Å; $V = 4589.6(3)$ $Å^3$; $Z = 8$; $D_{calc} = 1.791$ Mg m^{-3}; $\mu = 0.936$ mm^{-1}; $F(000) = 2464$. The final conventional R factor [R1, based on $|F|$ and 5751 data with $F > 4\sigma(F)$] was 0.0646, and weighted wR2 (based on F^2 and all 36 328 unique data from $\theta = 1.6-29.0°$) was 0.1534. The final ΔF synthesis extremes were +3.32 and −0.78 e $Å^{-}3$.

Crystal Data for Complex 5. Crystals suitable for X-ray diffraction were obtained by slow evaporation of an acetone/toluene solution at ambient temperature. The sample was a dark green lath of dimensions 0.76 × 0.46 × 0.16 mm^3: triclinic, space group $P\bar{1}$; $a = 8.2676(2)$ Å, $b = 12.2633(4)$ Å, $c = 12.8805(4)$ Å; $\alpha = 84.816(1)°$, $\beta = 83.151(1)°$, $\gamma = 80.501(1)°$; $V = 1275.50(7)$ $Å^3$; $Z = 2$; $D_{calc} = 1.672$ Mg m^{-3}; $\mu = 0.846$ mm^{-1}; $F(000) = 648$. The final conventional R factor [R1, based on $|F|$ and 5879 data with $F > 4\sigma(F)$] was 0.0484, and weighted wR2 (based on F^2 and all 12 210 unique data from $\theta = 1.6-28.9°$) was 0.1300. The final ΔF synthesis extremes were +2.00 and −1.70 e $Å^{-3}$.

NMR Spectroscopy. NMR spectra were recorded on either a Bruker DMX 500 MHz, AVA 600 MHz, or AVA 800 MHz spectrometers using TBI [^{1}H, ^{13}C, ^{15}N] probe-heads equipped with *z*-field gradients or on a Bruker DPX 360 MHz spectrometer. ^{1}H NMR signals were referenced to the residual solvent peak, δ 7.27 (chloroform), 2.07 (acetone), and 2.52 (DMSO), and for aqueous solutions (100% D_2O, 90% H_2O/10% D_2O) dioxan was added as an internal reference (δ 3.75). The water resonance was suppressed using a 1D double pulse field gradient spin−echo (DPFGSE) experiment. All spectra were recorded at 298 K unless stated otherwise, and data were processed using XWIN-NMR (Version 3.6 Bruker UK Ltd).

Elemental Analysis. Elemental analyses were carried out by either the University of Edinburgh using an Exeter analytical elemental analyzer CE440 or the University of St. Andrews using a Carlo Erba CHNS analyzer.

Electrospray Mass Spectrometry. ESI-MS were obtained on a Micromass Platform II mass spectrometer, and solutions were infused directly. The capillary voltage was 3.5 V, and the cone voltage used typically varied between 5 and 45 V. The source temperature was dependent on the solvent used.

UV−Vis Spectroscopy. A Perkin-Elmer Lambda-16 UV−vis spectrophotometer was used with 1 cm path length quartz cuvettes (0.5 mL) and a PTP1 Peltier temperature controller. Spectra were recorded at 298 K in water from 800 to 200 nm, unless otherwise stated, and were processed using UV-Winlab software for Windows 95.

ICP-OES. The ruthenium content of aqueous solutions was determined by ICP-OES at emission wavelengths of 240.272 and 349.894 nm (mean value of emission) using a Perkin-Elmer Optima 5300 DV ICP-OES machine calibrated with standard solutions (0.1−100 ppm).

pH Measurement. The pH values of aqueous solutions were measured at ca. 298 K using a Corning pH meter 240 equipped with an Thermo micro combination KCl or KNO_3 electrode calibrated with pH 4, 7, and 10 buffer solutions (Sigma-Aldrich). The pH meter readings for D_2O solutions were recorded without the correction for the effect of deuterium on the glass electrode and are termed pH*.

Determination of Molar Extinction Coefficients. The UV−vis spectra of the ruthenium compounds were recorded from 800 to 200 nm at five different concentrations, and the concentration of ruthenium was subsequently determined by ICP-OES. Linear plots of absorbance versus concentration gave the molar extinction coefficient as the gradient, according to the Beer−Lambert law $A = \epsilon cl$.

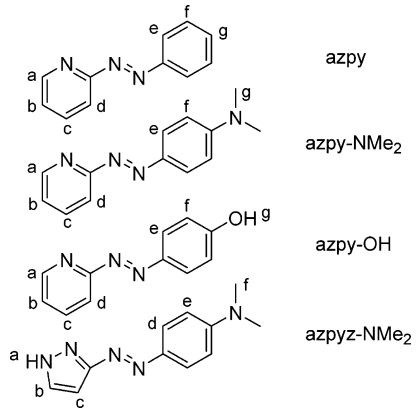

Figure 1. Molecular structure of chelating azo ligands, ligand abbreviations, and hydrogen numbering schemes.

Determination of pK_a* Values. The pH* values of NMR samples in D_2O were measured at 298 K directly in the NMR tube before and after recording NMR data to give an average pH* value. The pH* values were adjusted with NaOD and DCl or $HClO_4$. pK_a* values were determined by plotting the change in chemical shift against pH* and fitting the curve to the Henderson−Hasselbalch equation (eq 1) using the program KALEIDOGRAPH,[19] with the assumption that the observed chemical shifts are weighted averages of the populations of the protonated and deprotonated forms.

$$\delta_{obs} = \frac{\delta_{XH}[XH] + \delta_X[X]}{[XH] + [X]} \quad (1)$$

where δ_{obs} is the observed chemical shift, δ_{XH} the limiting chemical shift of the fully protonated form, and δ_X the limiting chemical shift of the deprotonated form.

The errors are estimated as ±0.05 pK units. pK_a* values were determined using the titration curves for a minimum of two ^{1}H resonances for each complex, and the mean value was taken. The proton resonances followed (see Figure 1 for labels) were Ha and Hc for azpy, Hf and Hg for azpy-NMe_2, Hb and Hf for azpy-OH, Ha and Hc for **9**, and Hg and CH_3 proton in *p*-cym arene for **13A**. For determination of the pK_a* value of aquated complex **13A**, complex **13** was dissolved in D_2O and 0.98 mol equiv of $AgPF_6$ was added. The solution was stirred for 24 h at 298 K, and AgCl was removed by filtration.

Rate of Hydrolysis of Complex 13. 13 was dissolved in methanol and diluted in acidified H_2O (pH adjusted to 2.27 by addition of $HClO_4$) to give a ca. 50 μM solution (95% H_2O, 5% MeOH). The absorbance was recorded at 3 min intervals at the selected wavelength over 24 h at 298 K. The measured pH of the solution was 2.21. A plot of the change in absorbance with time was fitted to the appropriate equation for pseudo-first-order kinetics using Origin version 7.5 (Microcal Software Ltd) to give the half-life and rate constant. The experiment was then repeated at 310 K on a fresh solution.

Rate of Arene Loss for Complexes 1 and 4. The complexes were dissolved in methanol and diluted with water to give ca. 100 μM solutions (95% H_2O, 5% MeOH). The absorbance was recorded

(19) *KALEIDAGRAPH*, version 3.09.; Synergy Software: Reading, PA, 1997.

at 3 min intervals at the selected wavelength over 24 h at 310 K. The pH values of the solutions were 6.03 (**1**) and 6.30 (**4**). Plots of the change in absorbance with time was fitted to the appropriate equation for pseudo-first-order kinetics using Origin version 7.5 (Microcal Software Ltd) to give the half-life and rate constant.

Rate of Decomposition of Complexes 5, 8, 9, and 12. The complexes were dissolved in 90% H_2O/10% D_2O to give concentrations of ca. 100 μM. The solutions were sonicated for ca. 10 min to ensure complete dissolution and then filtered. The pH was recorded (complex **5**, pH 6.60; complex **8**, pH 6.42; complex **9**, pH 5.14; and complex **12**, pH 5.46), and ^{1}H NMR spectra were recorded every hour for 12 (**9**), 14 (**5**) and (**8**), and 24 h (**9**) (and after 24 h for **9**, **5**, and **8**). The samples were kept at 310 K in a water bath between NMR data acquisitions. The percentage of species present in solution was determined by integration of the azo ligand Ha proton (see Figure 1) for the ligand present in the chloride, aqua and arene loss complexes. The data were fitted to the appropriate equation for pseudo-first-order kinetics using Origin version 7.5 or version 6.1 (Microcal Software Ltd) to give the approximate half-life and approximate rate constant.

Reaction of 13A with 9-Ethylguanine (9EtG). The aqua adduct **13A** was prepared by dissolving **13** in methanol-d_4 and diluting with D_2O to give a ca. 100 μM solution (95% D_2O, 5% MeOD), adding $AgPF_6$ (0.98 mol equiv), stirring the solution for 24 h at ambient temperature, and then filtering to remove AgCl. The pH* of the solution was adjusted to 7.42 by addition of NaOH/$HClO_4$ and then incubated at 310 K. To this solution 9EtG (ca. 100 μM, 95% D_2O, 5% MeOD, at 310 K) was added to give a 1:1 molar ratio of **13A** and 9EtG (50 μM) with a pH* of 7.46. The reaction of the two species was followed by ^{1}H NMR over 24 h with readings taken every hour. The extent of reaction of **13A** with 9EtG was determined by integration of azpyzNMe$_2$ Hb (see Figure 1) ^{1}H NMR peaks for **13A** and the 9EtG adduct.

Determination of IC_{50} Values. Compounds were tested for growth inhibitory activity against the A2780 and A549 cancer cell lines at six different concentrations (100, 50, 10, 5, 1, and 0.1 μM), each in triplicate. Cisplatin was also tested as a control. The A2780 cancer cell line was maintained by growing the cells in RPMI medium supplemented with 5% fetal bovine serum, 1% penicillin/streptomycin, and 2 mM L-glutamine. The A549 cancer cell line was maintained by growing the cells in DMEM medium supplemented with 10% fetal bovine serum, 1% penicillin/streptomycin, and 2 mM L-glutamine.

A2780 cancer cells were plated out at a density of 5000 cells/well (±10%) on day one. A549 cancer cells were plated out at a density 2000 cells/well (±10%) on day two. On day three, the test compound was dissolved in DMSO to give a stock solution of 20 mM, and serial dilutions were carried out in DMSO to give concentrations of complex in DMSO of 10, 2, 1, 0.2, and 0.02 mM. These were added to the wells to give the six test concentrations and a final concentration of DMSO of 0.5% (v/v). The wells were examined under the microscope to check for complete dissolution of the complex, and any precipitate present was noted. The cells were exposed to the complex for 24 h then, after removal of the complex, fresh medium was added and the cells were incubated for 96 h of recovery time. The remaining biomass was then estimated by the sulforhodamine B assay.[20] IC_{50} values were calculated using XL-Fit version 4.0 (IDBS, Surrey, UK).

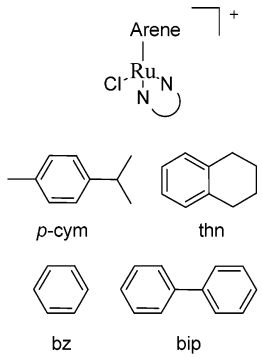

Compound	Arene	N-N
1	*p*-cym	azpy
2	thn	azpy
3	bz	azpy
4	bip	azpy
5	*p*-cym	azpy-NMe_2
6	thn	azpy-NMe_2
7	bz	azpy-NMe_2
8	bip	azpy-NMe_2
9	*p*-cym	azpy-OH
10	thn	azpy-OH
11	bz	azpy-OH
12	bip	azpy-OH
13	*p*-cym	azpyz-NMe_2
14	thn	azpyz-NMe_2
15	bz	azpyz-NMe_2
16	bip	azpyz-NMe_2

Figure 2. General structure of the complexes synthesized in this work as PF_6 salts.

Results

Sixteen chlorido Ru(II) arene complexes containing the chelated phenylazopyridine or phenylazopyrazole ligands azpy, azpy-OH, azpy-NMe_2, and azpyz-NMe_2 were synthesized and the structures of complexes **1**, **4**, and **5** were determined by X-ray crystallography. Electronic absorption spectra of the complexes in aqueous solution are reported and are compared to those of the free azo ligands. The pK_a* values of the pyridine conjugate acids of azpy, azpy-NMe_2, and azpy-OH have been determined. The aqueous solution chemistry of the complexes was investigated, mainly with respect to hydrolysis and arene loss, but also in relation to acidity of coordinated water (complex **13A**) and the phenolic OH (complex **9**). Finally, the cytotoxicity of these complexes toward the A2780 human ovarian and A549 human lung cancer cells was investigated.

Synthesis and Characterization. The chelating azo ligands used in this work are shown in Figure 1. They were synthesized according to previously published procedures[21−24] and were characterized by NMR and ESI-MS. The ruthenium arene complexes (Figure 2) were synthesized in good yields

(20) Skehan, P.; Storeng, R.; Scudiero, D.; Monks, A.; McMahon, J.; Vistica, D.; Warren, J. T.; Bokesch, H.; Kenney, S.; Boyd, M. R. *J. Natl. Cancer Inst.* **1990**, *82*, 1107−1112.

(21) Krause, R. A.; Krause, K. *Inorg. Chem.* **1980**, *19*, 2600−2603.
(22) Suminov, S. I. *Zh. Org. Khim.* **1968**, *4*, 1864−1865.
(23) Gorelik, M. V.; Lomzakova, V. I. *Zh. Org. Khim.* **1986**, *22*, 1054−1061.
(24) Betteridge, D.; John, D. *Analyst* **1973**, *98*, 377−389.

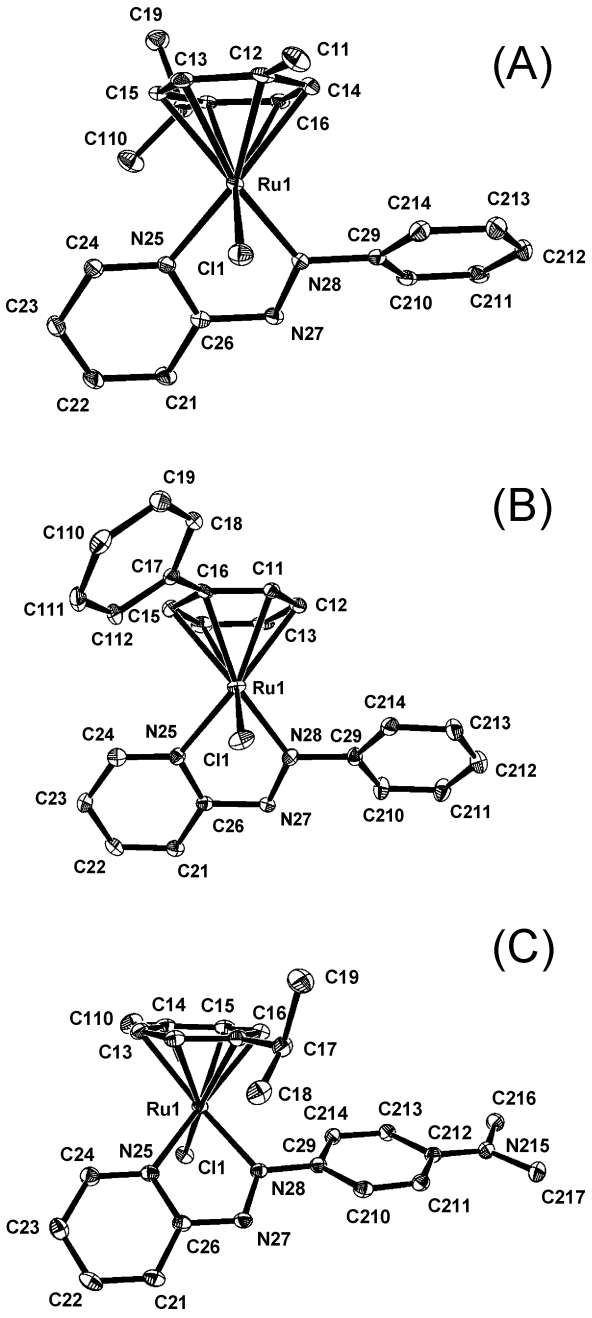

Figure 3. X-ray structures of the cations of (A) [(η^6-*p*-cym)Ru(azpy)Cl]-PF_6 (**1**), (B) [(η^6-bip)Ru(azpy)Cl]PF_6 (**4**), and (C) [(η^6-*p*-cym)Ru(azpy-NMe_2)Cl]PF_6 (**5**). Thermal ellipsoids show 30% probability. The hydrogen atoms have been omitted for clarity.

as PF_6 salts via the reaction of chloride-bridged dimers [(η^6-arene)$RuCl_2$]$_2$ and the chelating ligand in methanol. In general, the aqueous solubility of the complexes was low, ranging from between ca. 50 and 500 μM. The biphenyl complexes are the least soluble and benzene complexes the most soluble.

X-ray Crystallography. The molecular structures of the ruthenium complexes **1** and **5** were determined by single-crystal X-ray diffraction. The crystal structure of **4** was determined from a twinned crystal, which accounts for the slightly higher conventional *R* value of 6.46%. The structures along with their atom numbering schemes are shown in Figure 3A−C. Selected bond lengths and angles are listed in Table 1. The structures are similar, and complexes adopt the 'piano stool'-type geometry common to several other ruthenium(II) arene structures.[2,25] The ruthenium−arene centroid ring distances (**1**, 1.7203(16) Å; **4**, 1.707(2) Å; and **5**, 1.7107(15) Å) are longer than for analogous ruthenium-(II) arene complexes containing chelated ethylenediamine ligands (e.g., [(η^6-*p*-cym)Ru(en)Cl]PF_6, 1.6692(14) Å;[3] [(η^6-bip)Ru(en)Cl]PF_6, 1.662(3) Å).[25] It is interesting to note that the Ru(1)−N(28) azo bonds in these arene complexes, which range from 2.026(3) to 2.046(5) Å, are longer than in the crystal structures of Ru(II) phenylazopyridine structures α-[Ru(azpy)$_2$Cl$_2$], (1.977(4)−2.0084(4) Å), β-[Ru(azpy)$_2$Cl$_2$] (1.958(9)−2.003(9) Å), and γ-[Ru(azpy)$_2$Cl$_2$] (1.986(5)−1.988(5) Å).[6,26] Ru(1)−N(25) pyridine bond lengths, however, are within the same range as the [Ru(azpy)$_2$Cl$_2$] complexes. In all three structures, the Ru(1)−Cl(1) bond lengths (2.3704(9)−2.3830(15) Å) are comparable to other ruthenium(II) phenylazopyridine complexes but shorter than analogous ruthenium arene complexes containing the chelating ligand en, for which distances are in the range ca. 2.39−2.45 Å.[2,25]

Table 1. Selected Bond Lengths (Å) and Angles (deg) for [(η^6-*p*-Cym)Ru(azpy)Cl]PF_6 (**1**), [(η^6-bip)Ru(azpy)Cl]PF_6 (**4**), and [(η^6-*p*-Cym)Ru(azpy-NMe_2)Cl]PF_6 (**5**)

bond length/angle	**1**	**4**	**5**
Ru(1)−N(28)	2.026(3)	2.046(5)	2.040(3)
Ru(1)−N(25)	2.052(3)	2.067(5)	2.053(3)
Ru(1)−Cl(1)	2.3704(9)	2.3830(15)	2.3705(9)
Ru(1)−C(11)	2.256(4)	2.236(5)	2.263(3)
Ru(1)−C(12)	2.226(4)	2.238(6)	2.217(3)
Ru(1)−C(13)	2.220(4)	2.192(5)	2.221(3)
Ru(1)−C(14)	2.241(4)	2.170(6)	2.213(3)
Ru(1)−C(15)	2.181(4)	2.208(6)	2.176(4)
Ru(1)−C(16)	2.230(4)	2.254(6)	2.224(3)
Ru(1)−cent[a]	1.7203(16)	1.707(2)	1.7107(15)
N(27)−N(28)	1.280(4)	1.271(6)	1.290(4)
N(28)−Ru(1)−N(25)	75.41(12)	75.27(19)	75.61(11)

[a] Cent = centroid of η^6-arene.

Intermolecular $\pi-\pi$ stacking interactions are present in crystals of **1** between phenyl rings of the azo ligand, with arene centroid−centroid intermolecular distances of 3.732-(2) Å and an angle of 12.35° between the centroid−centroid vector and the vector normal to the plane of one of the rings. For complex **4**, all four aromatic rings are involved in stacking interactions with neighboring molecules (see Figure 4) with parameters listed in Table 2.

^{1}H NMR Spectroscopy. All synthesized ruthenium arene complexes were fully characterized by 1D ^{1}H NMR, 2D COSY, TOCSY, and 2D ROESY NMR methods. All complexes gave rise to similar NMR spectra, and a description of the ^{1}H NMR peak assignment strategy can be found in the Supporting Information (Figures S1 and S2). The OH and NH resonances were not observable in the ^{1}H NMR spectra. In general, the ^{1}H NMR resonances for the areneprotons of Ru(II) arene complexes are shifted downfield compared to the corresponding starting ruthenium dimers. For example, the *p*-cym proton resonances for complex **9**

(25) Chen, H.; Parkinson, J. A.; Parsons, S.; Coxall, R. A.; Gould, R. O.; Sadler, P. J. *J. Am. Chem. Soc.*. **2002**, *124*, 3064−3082.
(26) Seal, A.; Ray, S. *Acta Crystallogr., Sect. C* **1986**, *C42*, 1426−1428.

Table 2. Intermolecular $\pi-\pi$ Stacking Interaction Parameters for Complex **4**

ring(1)[a]	ring(2)[a]	distance[b] (Å)	angle[c] (deg)
$N_{25}-C_{24}-C_{23}-C_{22}-C_{21}-C_{26}$	$C_{29}-C_{210}-C_{211}-C_{212}-C_{213}-C_{214}$	3.958(3)	40.5
$C_{11}-C_{12}-C_{13}-C_{14}-C_{15}-C_{16}$	$C_{17}-C_{18}-C_{19}-C_{110}-C_{111}-C_{112}$	3.700(3)	20.18
$C_{17}-C_{18}-C_{19}-C_{110}-C_{111}-C_{112}$	$C_{11}-C_{12}-C_{13}-C_{14}-C_{15}-C_{16}$	3.701(3)	12.51
$C_{29}-C_{210}-C_{211}-C_{212}-C_{213}-C_{214}$	$N_{25}-C_{24}-C_{23}-C_{22}-C_{21}-C_{26}$	3.959(3)	17.08

[a] For atom numbering, see Figure 3B. [b] Centroid-to-centroid. [c] Between normal to the plane of ring(1) and ring(1)−ring(2) centroid-to-centroid vector.

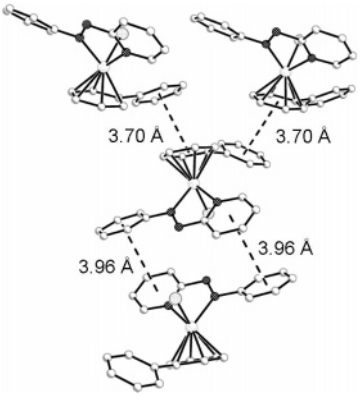

Figure 4. $\pi-\pi$ stacking interactions in crystals of [(η^6-bip)Ru(azpy)Cl]-PF_6 (**4**) (distances are centroid-to-centroid).

Table 3. Wavelengths of Maximum Absorbances, Extinction Coefficients, and Assignments for Azo Ligands in Methanol

ligand	λ_{max}/nm	ϵ/M^{-1} cm^{-1}	assignment
azpy	218	10 600	$\pi \rightarrow \pi^*$
	318	18 400	$\pi \rightarrow \pi^*$
	445	420	$n \rightarrow \pi^*$
azpy-NMe_2	272	10 700	$\pi \rightarrow \pi^*$
	432	35 900 (asym)[a]	$\pi \rightarrow \pi^*$
azpyz-NMe_2	267	12 200	$\pi \rightarrow \pi^*$
	402	33 000 (asym)[a]	$\pi \rightarrow \pi^*$
azpy-OH	246	10 000	$\pi \rightarrow \pi^*$
	358	25 200	$\pi \rightarrow \pi^*$

[a] Asymmetric peak.

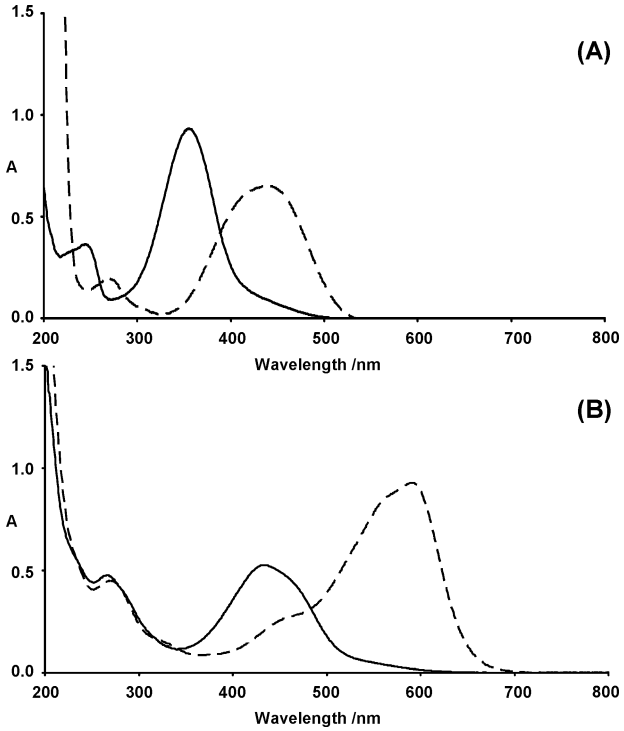

Figure 5. UV−vis spectra for aqueous solutions of (A) azpy-OH at pH ca. 7 (—) and ca. 13 (− − −), and (B) [(η^6-bip)Ru(azpy-OH)Cl]PF_6 (**12**, 42 μM) at pH ca. 2.5 (—) and ca. 10.5 (− − −), showing the dependence of $\pi \rightarrow \pi^*$ and MLCT transitions on pH.

are shifted downfield by ca. 0.6 ppm, thn resonances for complex **10** by ca. 0.5 ppm, biphenyl resonances for complex **11** by ca. 0.2 ppm, and benzene resonance for complex **12** by ca. 0.2 ppm.

Electronic Absorption Spectroscopy of Ligands. The wavelengths and intensities of the bands in the electronic absorption spectra of the free azo ligands in methanol are summarized in Table 3. Each free ligand exhibits a $\pi \rightarrow \pi^*$ transition[27] above 300 nm centered primarily on the azo group, and the ϵ_{max} of this band shifts to longer wavelengths with increasing σ-donating ability of the para substituent on the benzene ring (NMe_2 > OH > H), and on changing the heterocycle from pyrazole to pyridine, i.e., ϵ_{max} azpy-NMe_2, 432 nm; azpyz-NMe_2, 402 nm; azpy-OH, 358 nm; and azpy, 318 nm. The peaks below 300 nm are also tentatively assigned to $\pi \rightarrow \pi^*$ transitions. Azpy displays a weak $n \rightarrow \pi^*$ (forbidden) transition at 445 nm, and while this transition was not observed for the other ligands, it may be masked by the intense $\pi \rightarrow \pi^*$ transitions.

The effect of deprotonation of the OH group in azpy-OH on the UV−vis spectrum was investigated. Figure 5A compares the UV−vis spectrum of azpy-OH in water at ca. pH 7 and 13. Upon deprotonation of azpy-OH, the $\pi \rightarrow \pi^*$ transitions shift from 246 and 358 to 268 and 435 nm. This shift to longer wavelength correlates with the increased σ-donation from O^- vs OH into the benzene ring of the ligand.

Electronic Absorption Spectroscopy of Ruthenium Complexes. The wavelengths and intensities of the bands in the electronic absorption spectra of fresh aqueous solutions of the ruthenium complexes containing azpy, azpy-NMe_2, and azpyz-NMe_2 are summarized in Table 4, and those for azpy-OH and its corresponding deprotonated form in Table 5. All complexes display intense transitions in the visible region assignable to MLCT (metal−ligand charge transfer) from the filled 4d orbitals of Ru(II) to the empty π^* ligand orbitals ($4d^6$ Ru $\rightarrow \pi^*$). Both the position and the intensity of these transitions are highly dependent on the chelating ligand. For example, the effect on the UV−vis spectrum of changing the chelating ligand in ruthenium *p*-cym complexes

(27) The assignment of this transition (as $\pi \rightarrow \pi^*$) was confirmed by solvent effects. Upon changing solvent from methanol to 90% water/10% methanol the transition shifted to a longer wavelength. In contrast, $n \rightarrow \pi^*$ transitions are characteristically shifted to shorter wavelengths with increasing solvent polarity: Lambert, J. B.; Shurvell, H. F., Lightner, D. A., Cooks, R. G. *Organic Structural Spectroscopy*; Prentice Hall, Inc: New York, 1998.

Table 4. Wavelengths of Maximum Absorbance, Extinction Coefficients, and Assignments for Ru(II) Arene Complexes Containing Ligands Azpy, Azpy-NMe_2, and Azpyz-NMe_2 in Water

compound	λ_{max}/nm	ϵ/M^{-1} cm^{-1}	assignment[b]
1	262	9500	IL $\pi \rightarrow \pi^*$
	370	18 000	IL $\pi \rightarrow \pi^*$
	471	6000	Ru ($4d^6$) $\rightarrow \pi^*$
2	268	9500	IL $\pi \rightarrow \pi^*$
	368	17 100	IL $\pi \rightarrow \pi^*$
	471	5900	Ru ($4d^6$) $\rightarrow \pi^*$
3	359	12 200	IL $\pi \rightarrow \pi^*$
	465	4000	Ru ($4d^6$) $\rightarrow \pi^*$
4	269	14 100	IL $\pi \rightarrow \pi^*$
	364	14 000	IL $\pi \rightarrow \pi^*$
	470	5000	Ru ($4d^6$) $\rightarrow \pi^*$
5	294	10 000	IL $\pi \rightarrow \pi^*$
	457	9100	IL $\pi \rightarrow \pi^*$
	584	36 000 (sh)[a]	Ru ($4d^6$) $\rightarrow \pi^*$
	626	42 700	Ru ($4d^6$) $\rightarrow \pi^*$
6	296	15 300	IL $\pi \rightarrow \pi^*$
	458	13 400	IL $\pi \rightarrow \pi^*$
	584	39 400 (sh)[a]	Ru ($4d^6$) $\rightarrow \pi^*$
	627	46 700	Ru ($4d^6$) $\rightarrow \pi^*$
7	295	10 000	IL $\pi \rightarrow \pi^*$
	452	8200	IL $\pi \rightarrow \pi^*$
	584	38 700 (sh)[a]	Ru ($4d^6$) $\rightarrow \pi^*$
	620	44 200	Ru ($4d^6$) $\rightarrow \pi^*$
8	295	13 100	IL $\pi \rightarrow \pi^*$
	452	11 000	IL $\pi \rightarrow \pi^*$
	584	53 700 (sh)[a]	Ru ($4d^6$) $\rightarrow \pi^*$
	621	63 700	Ru ($4d^6$) $\rightarrow \pi^*$
13	302	8900	IL $\pi \rightarrow \pi^*$
	469	14 300	IL $\pi \rightarrow \pi^*$
	577	22 100	Ru ($4d^6$) $\rightarrow \pi^*$
14	303	7800	IL $\pi \rightarrow \pi^*$
	481	11 900	IL $\pi \rightarrow \pi^*$
	581	22 500	Ru ($4d^6$) $\rightarrow \pi^*$
15	303	8000	IL $\pi \rightarrow \pi^*$
	469	13 200	IL $\pi \rightarrow \pi^*$
	573	20 600	Ru ($4d^6$) $\rightarrow \pi^*$
16	295	12 800	IL $\pi \rightarrow \pi^*$
	481	13 000	IL $\pi \rightarrow \pi^*$
	592	25 700	Ru ($4d^6$) $\rightarrow \pi^*$

[a] sh = shoulder. [b] IL = Intraligand.

is shown in Figure 6. The wavelength of the MLCT increases from azpy-OH (469 nm) ≈ azpy (471 nm) < azpyz-NMe_2 (577 nm) < azpy-NMe_2 (626 nm). This increase in wavelength is also accompanied by an increase in the molar extinction coefficient, i.e., **1** (6000 M^{-1} cm^{-1}) < **9** (7000 M^{-1} cm^{-1}) < **13** (22 100 M^{-1} cm^{-1}) < **5** (42 700 M^{-1} cm^{-1}). There are also small differences in both the position and the intensity of the MLCT bands when the arene is changed for a given series with the same chelating ligand. There appears, however, to be no simple correlation between the position and intensity of the MLCT band and the arene. The UV−vis spectra of these ruthenium complexes also display similar intraligand $\pi \rightarrow \pi^*$ transitions to those in the free ligands but they are shifted to longer wavelengths for the complexes.

The complexes containing the azpy-OH ligand display interesting pH-dependent spectra. The UV−vis spectra for all complexes at pH 2.5, where the ligand is fully protonated, display a MLCT band at ca. 469 nm (ϵ = 7000−8600 M^{-1} cm^{-1}). This transition is partially obscured by the intraligand $\pi \rightarrow \pi^*$ transitions. Raising the pH of the aqueous solutions to ca. 10.5 led to deprotonation of the azpy-OH ligand and dramatically changed the UV−vis spectrum. For

Table 5. Wavelengths of Maximum Absorbance, Extinction Coefficients, and Assignments for Ru(II) Arene Complexes Containing Protonated Azpy-OH or Deprotonated Azpy-O^- in Water[a]

compound	λ_{max}/nm	ϵ/M^{-1} cm^{-1}	assignment
9 (OH)	264	5100	IL $\pi \rightarrow \pi^*$
	432	9500	IL $\pi \rightarrow \pi^*$
	469	7000 (sh)	Ru ($4d^6$) $\rightarrow \pi^*$
9 (O^-)	280	4600	IL $\pi \rightarrow \pi^*$
	457	4900 (sh)	IL $\pi \rightarrow \pi^*$
	560	15 100	Ru ($4d^6$) $\rightarrow \pi^*$
	588	15 600	Ru ($4d^6$) $\rightarrow \pi^*$
10 (OH)	267	5600	IL $\pi \rightarrow \pi^*$
	430	10 200	IL $\pi \rightarrow \pi^*$
	469	7600 (sh)	Ru ($4d^6$) $\rightarrow \pi^*$
10 (O^-)	280	4800	IL $\pi \rightarrow \pi^*$
	460	5100 (sh)	IL $\pi \rightarrow \pi^*$
	563	16 700	Ru ($4d^6$) $\rightarrow \pi^*$
	587	16 500	Ru ($4d^6$) $\rightarrow \pi^*$
11 (OH)	260	5800	IL $\pi \rightarrow \pi^*$
	429	11 100	IL $\pi \rightarrow \pi^*$
	469	8000 (sh)	Ru ($4d^6$) $\rightarrow \pi^*$
11 (O^-)	278	5700	IL $\pi \rightarrow \pi^*$
	454	5600 (sh)	IL $\pi \rightarrow \pi^*$
	557	18 900	Ru ($4d^6$) $\rightarrow \pi^*$
	587	19 900	Ru ($4d^6$) $\rightarrow \pi^*$
12 (OH)	267	9900	IL $\pi \rightarrow \pi^*$
	430	10 800	IL $\pi \rightarrow \pi^*$
	469	8600 (sh)	Ru ($4d^6$) $\rightarrow \pi^*$
12 (O^-)	269	9100	IL $\pi \rightarrow \pi^*$
	457	5500 (sh)	IL $\pi \rightarrow \pi^*$
	561	17 400	Ru ($4d^6$) $\rightarrow \pi^*$
	591	19 000	Ru ($4d^6$) $\rightarrow \pi^*$

[a] (sh) = shoulder, IL = intraligand.

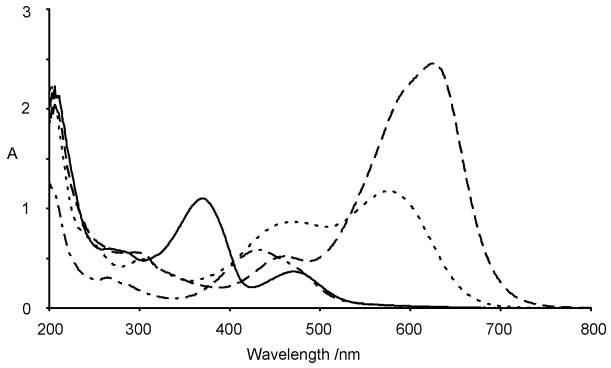

Figure 6. UV−vis spectra for fresh aqueous solutions of [(η^6-*p*-cym)Ru(azpy)Cl]PF_6 (**1**, 58 μM, —), [(η^6-*p*-cym)Ru(azpy-NMe_2)Cl]PF_6 (**5**, 54 μM, − − −), [(η^6-*p*-cym)Ru(azpy-OH)Cl]PF_6 (**9**, 49 μM, − - −), and [(η^6-*p*-cym)Ru(azpyz-NMe_2)Cl]PF_6 (**13**, 56 μM, - - -) showing the effect of variations in the azo ligand on the absorption spectrum.

example, the MLCT band of **12** shifts from 469 to ca. 588 nm with a shoulder at ca. 560 nm (Figure 5B). For these deprotonated forms, the extinction coefficient increases to between 15 100 and 18 900 M^{-1} cm^{-1}. The intense intraligand $\pi \rightarrow \pi^*$ transitions also shift to longer wavelengths (to ca. 277 and 457 nm).

Determination of pK_a* Values. The variation in ^{1}H NMR chemical shifts with pH* allowed determination of the pK_a* values for the ionisable groups of the chelating phenylazopyridine ligands, as well as for the deprotonation of the phenolic OH in complex **9** and the coordinated water in complex **13A**.

Phenylazopyridine Ligands. The pK_a* values for the conjugate acids of the pyridine nitrogens of the free ligands were determined as 2.47 for azpy, 3.06 for azpy-OH, 4.60

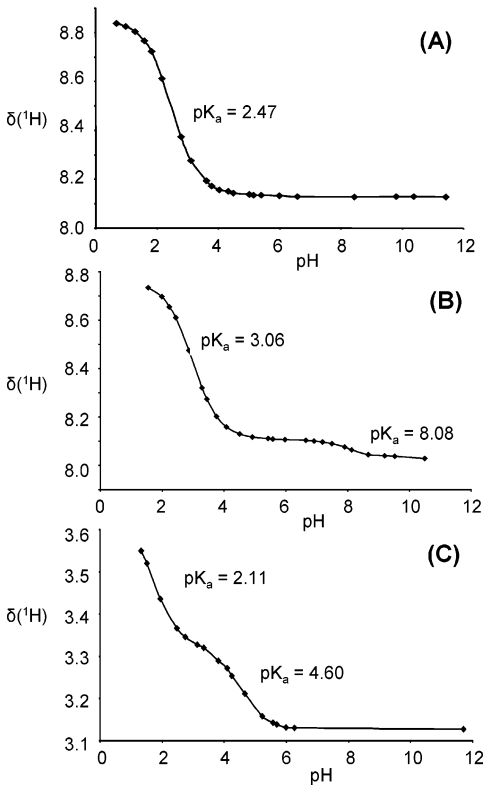

Figure 7. Dependence of the ^{1}H NMR chemical shifts on pH for (A) azpy, (B) azpy-NMe$_2$, and (C) azpy-OH. The curves represent best fits to the Henderson−Hasselbalch equation giving pK_a values of 2.47 for azpy, 3.06 for azpy-OH, and 4.60 for azpy-NMe$_2$.

for azpy-NMe$_2$, and for the OH of azpy-OH 8.08, and NHMe$_2^+$ in azpy-NMe$_2$ 2.11 (Figure 7).

Phenolic Group in 9. A pK_a* value of 6.48 was determined for deprotonation of the phenol group of azpy-OH in complex **9** (Figure S3).

Coordinated Water in 13A. A pK_a* value of 4.5 was determined for the coordinated water in the aqua adduct **13A** (Figure S4).

Aqueous Solution Chemistry. The aqueous solution chemistry (with respect to hydrolysis and arene loss) of complexes **1**, **4**, **5**, **8**, **9**, **12**, and **13** was studied at 310 K over 24 h. The aqueous solubility of complex **16** was too low to allow such studies. In general, the complexes were found to undergo a mixture of slow hydrolysis and arene loss (to give products in which the three coordination sites originally occupied by the arene are now occupied by solvent). Exchange between species present in solution was slow on the NMR time scale; separate sets of peaks were observed for the chlorido, aqua, and arene-loss species (see Figure 8). Hydrolysis was confirmed by adding excess NaCl (100 mM) and noting the decrease in the intensity of the aqua peaks as the water is replaced by chloride. Arene loss was inferred by the presence of resonances for free *p*-cym (ca. δ 7.23 (dd)) and free biphenyl (ca. δ 7.9 (d), 7.70 (t), 7.45 (t)) in the aromatic region of the ^{1}H NMR spectra.

The speciation after 24 h was first determined by ^{1}H NMR for the complexes studied (Table 6). For example, Figure 8 shows the ^{1}H NMR spectrum of **5** initially (after 35 min) and after 24 h incubation in 90% H_2O/10% D_2O at 310 K.

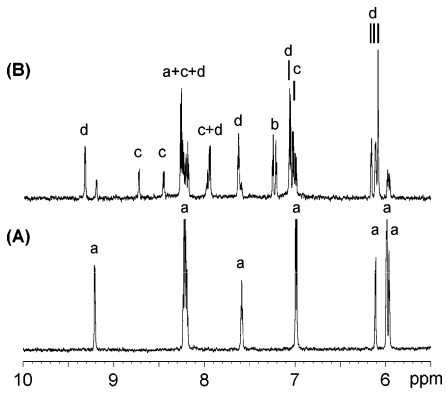

Figure 8. ^{1}H NMR spectra of **5** in 90%H_2O/10%D_2O (A) at 310 K 35 min after dissolution and (B) at 310 K 24 h after dissolution. Peak assignments: **a**, intact chlorido complex **1**; **b**, free *p*-cymene; **c**, a ruthenium phenylazopyridine complex after arene loss; and **d**, aquated **5**.

Table 6. Hydrolysis and Stablility of Complexes of [(η^6-*p*-cym)Ru(azpy)Cl]PF$_6$ (**1**), [(η^6-bip)Ru(azpy)Cl]PF$_6$ (**4**), [(η^6-*p*-cym)Ru(azpy-NMe$_2$)Cl]PF$_6$ (**5**), [(η^6-bip)Ru(azpy-NMe$_2$)Cl]PF$_6$ (**8**), [(η^6-*p*-cym)Ru(azpy-OH)Cl]PF$_6$ (**9**), [(η^6-bip)Ru(azpy-OH)Cl]PF$_6$ (**12**), and [(η^6-*p*-cym)Ru(azpyz-NMe$_2$)Cl]PF$_6$ (**13**)

			% species (24 h, 310 K)		
complex	$k_{(obs)}$/h^{-1a}	$t_{1/2}$/h	intact	hydrolyzed	arene loss
1	0.0601^b (±0.0004)	11.55	50	0	50
4	0.0782^b (±0.0007)	8.87	33	0	67
5	0.078^c (±0.014)	8.90	23	55	22
8	0.034^c (±0.007)	20.27	24	9	67
9	0.033^c (±0.006)	21.03	36	34	30
12	0.053^c (±0.007)	13.05	31	5	64
13	0.3233^d (±0.0004)	2.14	5	95	0

^{a} The errors quoted are fitting errors. ^{b} Determined by UV−vis spectroscopy for a 100 μM solution in 95% H_2O, 5% MeOH. ^{c} Determined by ^{1}H NMR spectroscopy in 90% H_2O, 10% D_2O by following the decomposition of the intact complex with time. ^{d} Determined by UV−vis spectroscopy for a 50 μM solution in 95% H_2O, 5% MeOH

The initial ^{1}H NMR spectrum of **5** contained one set of peaks (species **a** in Figure 8A). After 24 h this species still accounted for 23% (based on peak integrals) and was assigned as the intact chlorido complex. There were three new species present after the 24 h of incubation, (Figure 8B): species **b** (free *p*-cymene), **c** (phenylazopyridine Ru(II) complex formed after loss of arene) which accounted for 22%, and a third species **d** (ca.55%) assignable to [(η^6-*p*-cym)Ru(Azpy-NMe$_2$)(H_2O/OH)]$^{2+/1+}$. Figure S5 shows the 2D TOCSY ^{1}H NMR spectrum after 24 h, which aided the assignment of peaks.

For the complexes that underwent only one process, as detected by ^{1}H NMR spectroscopy (complex **13** hydrolysis, complexes **1** and **4** arene loss), the rate of this process was then determined by UV−vis spectroscopy. For the complexes undergoing both arene loss and hydrolysis, the initial rate of disappearance of the intact complex was determined by ^{1}H NMR spectroscopy. The rate data are summarized in Table 6.

Rate of Aquation of 13. The time dependence of the absorption spectrum for an aqueous solution of **13** (ca. 50 μM, pH 2.21, 95% H_2O, 5% MeOH) is shown in Figure S6. The presence of isosbestic points at 430 and 520 nm suggests a single step reaction from the initial chlorido complex to aqua product at this pH. The maximum change in absorbance

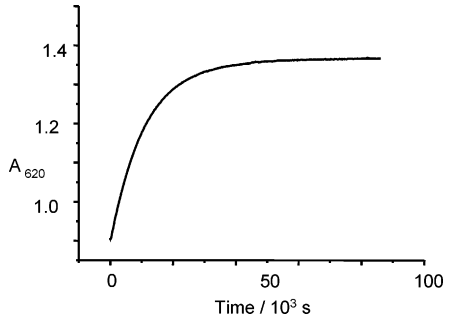

Figure 9. Dependence of the absorbance at 620 nm over 24 h during aquation of complex **13** at 310 K.

occurred at 620 nm, and this wavelength was chosen for the kinetic study. Figure 9 shows the variation in the absorbance at 620 nm with time at 310 K over 24 h. This change in absorbance followed pseudo-first-order kinetics, giving a rate constant $k_{obs} = 0.3233$ (± 0.0004) h^{-1} and a half-life of $t_{1/2} = 2.14$ h. This experiment was repeated at 298 K (to allow comparison with rate data of other Ru(II) arenes), giving $k_{obs} = 0.0870$ (± 0.0001) h^{-1} and a half-life of $t_{1/2} = 8.17$ h (Figure S7).

Rate of Arene Loss for 1 and 4. The rates of arene loss for complexes **1** and **4** were determined by a similar procedure. Figure S8 shows the variation in the absorbance at 375 nm with time at 310 K over 24 h for complex **1**, and Figure S9 shows the variation in the absorbance at 399 nm with time at 310 K over 24 h for complex **4**. The rate of arene loss from the *p*-cym complex **1** ($t_{1/2} = 11.55$ h^{-1}) was slightly slower than for bip complex **4** ($t_{1/2} = 8.87$ h^{-1}), Table 6.

Rate of Reaction of 5, 8, 9, and 12. Figure 10 shows the disappearance of the starting chlorido complexes **5**, **8**, **9**, and **12** and formation of aquated and arene-loss products over time as determined from ^{1}H NMR integrals. The rate of disappearance of the chlorido complexes appeared to follow pseudo-first-order kinetics and gave the rate constants and associated half-lives shown in Table 6. Complexes **8** and **9** reacted very slowly ($t_{1/2} > 20$ h), whereas complexes **5** and **12** reacted somewhat faster ($t_{1/2} = 9-13$ h).

Table 7. IC_{50} Values for Ru(II) Arene Complexes Against the A2780 Human Ovarian and A549 Human Lung Cancer Cell Lines and Comparison with Cisplatin

	IC_{50} (μM)			IC_{50} (μM)	
complex	A2780	A549	complex	A2780	A549
1	>100	>100	**9**	58	>100
2	>100	>100	**10**	34	63
3	>100	>100	**11**	>100	>100
4	>100	>100	**12**	18	56
5	>100	>100	**13**	18	41
6	>100	>100	**14**	57	>100
7	>100	>100	**15**	88	>100
8	44	49	**16**	24	32
cisplatin	5	5			

Reaction of 13A with 9EtG. The reaction between **13A** and 1 mol equiv of 9EtG at pH* 7.46 was followed by ^{1}H NMR spectroscopy. The aqua adduct is predominantly in the hydroxo form at this pH* ($pK_a^* = 4.60$ vide supra). The reaction reached equilibrium after ca. 10 h when ca. 28% of the 9EtG was bound to ruthenium. Figure S10 shows the variation in time in the amount of **13A** which reacted with 9EtG (based on integration of azopyrazole ^{1}H NMR peaks).

Cytotoxicity. The IC_{50} values for complexes **1**−**16** against the A2780 human ovarian and A549 human lung cancer cell lines are given in Table 7. All complexes appeared to be soluble at the testing concentrations with the exception of complex **16** at 100 μM. However, none of the cells survived even at 50 μM of **16**. The compounds were initially dissolved

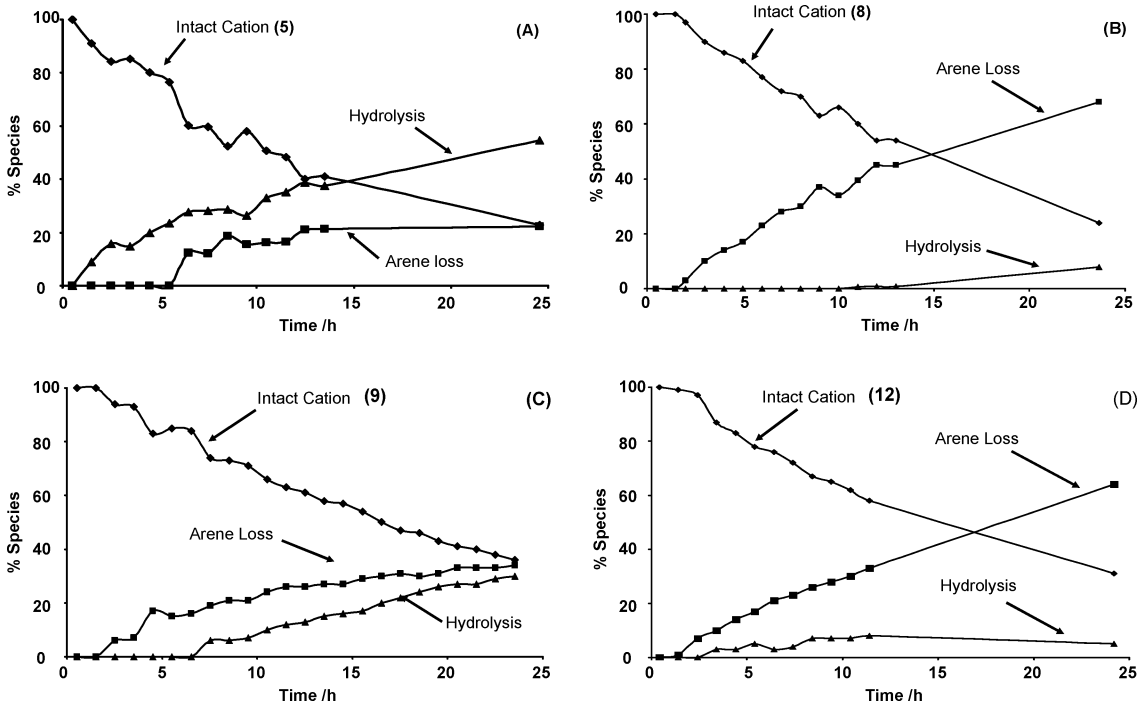

Figure 10. Percentage of species present over 24 h for 100 μM solutions of (A) complex **5**, (B) complex **8**, (C) complex **9**, and (D) complex **12** as determined by the ratio of the integrals of the Ha proton (see Figure 1) of the phenylazo ligand in the different environments.

in DMSO and diluted with cell media within 30 min (to give a DMSO concentration of 0.5% v/v).

None of the Ru(II) arene complexes with the chelating azo ligand azpy (**1**−**4**) were cytotoxic to either cell line, and of the complexes containing azpy-NMe_2 (**5**−**8**), only the bip complex **8** was cytotoxic in both the A2780 and A549 cell lines with IC_{50} values of ca. 45 μM. All the complexes containing the azpyz-NMe_2 (**13**−**16**) ligand exhibit cytotoxicity against the A2780 cancer cell line, the most potent being the *p*-cym and bip complexes, which also displayed good cytotoxicity in the A549 cell line. With the exception of the benzene complex **11**, all Ru complexes containing azpy-OH exhibited activity against the A2780 cancer cell line, with **10** and **12** also displaying moderate cytotoxicity against A549 cancer cells. The cytotoxicity observed in the A2780 cancer cell line is markedly lower than that for analogous Ru(II) arenes with en as the chelating ligand, for which values lie in the range of $IC_{50} = 10$ μM for [(η^6-p-cym)Ru(en)Cl]PF_6 and $IC_{50} = 5$ μM for [(η^6-bip)Ru(en)Cl]PF_6.[2]

Discussion

In the literature there are several examples of ruthenium azpy complexes (vide supra), but there appear to be no reports of ruthenium complexes containing the chelated ligands azpy-NMe_2, azpy-OH, or azpyz-NMe_2. Furthermore, to the best of our knowledge, this report contains the first example of azpyz-NMe_2 being used as a chelating ligand for any metal.

The introduction of chelating azopyridine and azopyrazole ligands into chlorido Ru(II) arene complexes has given rise to highly colored complexes, which exhibit new properties in comparison with complexes containing diamines such as en as chelating ligands; the rate of hydrolysis decreases, arene loss acts as a competing reaction, the pK_a* of the coordinated water decreases, and affinity for DNA appears to be lowered, yet despite these differences, the azo complexes still exhibit moderate cytotoxicity against the A2780 and A549 cancer cells.

Structures of Complexes. The relatively long Ru−N(28) azo bonds in the X-ray crystal structures of azopyridine complexes **1**, **4**, and **5** can be ascribed to back-bonding competition for the ruthenium $4d^6$ electron density by the azopyridine and arene π-acceptor ligands. Such an effect has also been observed in the crystal structure of [$Ru(azpy)_3$]-$(PF_6)_2$.[12] Further evidence for such competition in complexes **1**, **4**, and **5** is the lengthening of the Ru−arene centroid distances by ca. 0.04 Å compared to analogous ruthenium-(II) arenes with ethylenediamine as the chelating ligand (a non-π-acceptor).

The phenyl−phenyl and phenyl−pyridyl $\pi-\pi$ intermolecular interactions all fall within the commonly observed range for stacks of aromatic groups, with approximately parallel planes, separation distances of 3.3−3.8 Å, and angles between the normal to one ring and the centroid vector of ca. 16−40°.[28] Polarization of the phenyl ring of the ligand in **1** and **4** by the electron-withdrawing azo group is likely to enhance its ability to stack. Similarly, the π-electron deficiency of the pyridine ring in **4** is also likely to favor stacking.

The ability of the η^6-arene to stabilize Ru(II) by π-acceptor interactions[29] is evident from the ^{1}H NMR resonances of the metal-coordinated η^6-arenes. These are shifted upfield due to increased electron density on the ring, compared with the uncoordinated arene.[30] It is noteworthy that the protons of the η^6-arenes in the azo compounds studied in this work are deshielded (by between 0.2 and 0.6 ppm) compared to the corresponding starting dimers [(η^6-arene)$RuCl_2$]$_2$. This is consistent with a reduced electron density in the arene ring upon chelation of the azo ligand to ruthenium, indicating that the π-accepting arene and π-accepting azo ligand compete for Ru electron density.

Electronic Absorption Spectroscopy. The major differences in the UV−vis spectra with changes in the chelating ligand can be rationalized as follows. For the complexes containing phenylazopyridine ligands, the introduction of electron-donating groups on to the phenyl ring (O^- in azpy-O^- and NMe_2 in azpy-NMe_2) decreases the π-acidity of the azo group[31] which causes an increase in the energy of the Ru(II) $4d^6$ orbitals and results in a smaller energy gap between the Ru $4d^6$ bonding and azo π* orbitals. This is manifested in the spectrum as a progressive shift of the MLCT band to longer wavelengths with increased σ-donor strengths of the phenyl substituents on the ligand. The replacement of pyridine by pyrazole as a substituent results in a decrease in the wavelength of the MLCT, presumably the azopyrazole π* orbital must be at a higher energy.

Acidity of Ligands and Complexes. Phenylazopyridine Ligands. The pK_a* values (of the conjugate acids) of the pyridine nitrogens for the free azo ligands are 2.77 (azpy), 2.18 (azpy-OH), and 0.64 (azpy-NMe_2) pK_a units lower than for pyridine itself (5.24).[32] This is attributed to the electron-withdrawing effects of the azo group, which serves to reduce their basicity.[33] The presence of the NMe_2 and, to a lesser extent, the OH substituent on the phenyl ring increases the basicity of the pyridine nitrogen relative to azpy (H) due to electron donation by the dimethylamino/hydroxyl groups, which opposes the electron-withdrawing effect of the azo group on the pyridyl ring.[34] The relatively low pK_a* values for the pyridyl ligands suggest that they are poor σ-donors, compared with, for example ethylenediamine, $pK_{a1} = 7.08$ and $pK_{a2} = 9.89$.[32] Pyridine is a six-membered π-electron deficient ligand and, besides being a σ-donor, can also act as a π-acceptor toward Ru(II). The pyridine ring in azpy is expected to be a better π-acceptor than the pyridine ring in azpy-NMe_2 since it is more electron deficient. Thus, overall,

(28) Janiak, C. *J. Chem. Soc., Dalton Trans.* **2000**, 3885−3896.
(29) Bennett, M. A.; Brines, M. J.; Kovacik, I. *J. Organomet. Chem.* **2004**, *689*, 4463−4474.
(30) Stebler-Roethlisberger, M.; Hummel, W.; Pittet, P. A.; Buergi, H. B.; Ludi, A.; Merbach, A. E. *Inorg. Chem.* **1988**, *27*, 1358−1363.
(31) Krause, R. A.; Krause, K. *Inorg. Chem.* **1984**, *23*, 2195−2198.
(32) Kotrlý, S.; Šùcha, L. *Handbook of Chemical Equilibria in Analytical Chemistry*; Ellis Horwood Ltd: Chicester, 1985.
(33) Ackermann, M. N.; Fairbrother, W. G.; Amin, N. S.; Deodene, C. J.; Lamborg, C. M.; Martin, P. T. *J. Organomet. Chem.* **1996**, *523*, 145−151.
(34) Pentimalli, L. *Tetrahedron* **1960**, *9*, 194−201.

azpy would be expected to give rise to a higher positive charge on Ru(II)/lower electron density on Ru(II), compared to azpy-OH and azpy-NMe_2 since it is a weaker σ-donor and a stronger π-acceptor. Correlations between the substituents on pyridine rings and metal pyridine π-bonding have been discussed previously in the literature.[35,36]

Phenol Group in azpy-OH and Complex 9. The pK_a* of the phenol group of azpy-OH in complex **9** (6.48) is 1.6 pK_a units lower than that in the free ligand. This suggests that electron density from the phenolate group is more readily delocalized when azpy-O^- is coordinated to Ru. At physiological pH (7.4), the compound will exist predominantly in the deprotonated form, and so the complex will bear no overall charge.

Aqueous Solution Chemistry. The complexes studied undergo a combination of hydrolysis and arene loss in water. Reactions are slow, with half-lives of the order of hours at 310 K (body temperature). In general, for the biphenyl complexes, arene loss predominates over hydrolysis with little hydrolysis observed over 24 h for complexes **4**, **8**, and **12**. For the *p*-cym complexes, as the pK_a* of the pyridine nitrogen increases, a reduced amount of arene loss and increased amount of hydrolysis is observed, e.g., for complexes **5** and **9** compared with **1**. Thus, increased electron density at Ru(II) facilitates the substitution of chloride by water and disfavors arene loss.

The rates of ligand substitution in hexacoordinated Ru(II) complexes are known to span about 10 orders of magnitude.[37] The trend in rates correlates with the extent of back-bonding[38] from moderately fast exchange for non-π-acceptor ligands (e.g., $[Ru(H_2O)_6]^{2+}$) to very inert behavior with π-acceptor ligands (e.g., $[Ru(MeCN)_6]^{2+}$). The inertness results from the high thermodynamic stability of the starting complex due to π back-bonding from Ru(II) $4d^6$ to the π* orbital of MeCN. The presence of both the arene and the azo ligand in the complexes studied here would be expected to give rise to more slowly reacting compounds.

Arene Loss. For the ruthenium phenylazopyridine complexes studied, biphenyl is a more labile arene than *p*-cym. For example, the amount of arene loss from **1** is 50% after 24 h compared with 67% for **4** and the rate of arene loss is ca. 30% faster in the biphenyl case, ($t_{1/2}$ 8.87 h (**4**) compared with 11.55 h (**1**)). The presence of electron-donating alkyl groups on the bound arene strengthens the ruthenium−arene bond[39] and therefore should make *p*-cym a less labile arene than bip.

In the literature there are several examples of the photochemical displacement of an η^6-arene from Ru[40] but thermal displacement, especially under such mild conditions (low temperatures, aqueous solution), is uncommon, and most displacements occur in the presence of strong nucleophiles, these reactions still being relatively rare.[41] The observed loss of arene in aqueous solution can be rationalized by considering the nature of the bonding of an η^6-arene to Ru(II), which is strengthened by π-back-donation from the ruthenium center. In the azopyridine complexes, the arene is less tightly bound to ruthenium due to competition with the azo ligand for π-electron density.

Hydrolysis. The chlorido complexes **5**, **9**, and **13** all undergo hydrolysis, although for **5** and **9**, arene loss is a competing reaction whereas this is not the case for **13**. Thus, there is a marked difference in aqueous solution chemistry between **5** and **13** on changing the chelating ligand from an azopyridine to azopyrazole. Complex **13** undergoes more extensive and more rapid hydrolysis than **5** with no arene loss (Table 6). Pyridine is a π-electron-deficient heterocycle, functioning as a σ-donor/π-acceptor ligand, whereas pyrazole is formally classed as a five-membered π-electron-rich heterocycle[42] and binds to metals primarily in a σ-donor fashion. The lack of π-back-bonding ability of pyrazole has been noted in the literature.[43] Thus, azpyz-NMe_2 is a less efficient π-acceptor ligand, resulting in a subsequent increase in chloride lability and a decrease in arene lability.

Rate of Hydrolysis of 13. The half-lives for aquation of the chlorido ethylenediamine ruthenium(II) arene complexes, $[(\eta^6\text{-dha})Ru(en)Cl]^+$, $[(\eta^6\text{-tha})Ru(en)Cl]^+$, and $[(\eta^6\text{-bip})Ru(en)Cl]^+$, (dha = dihydroanthracene, tha = tetrahydroanthracene) have been reported to be 4.3−9.4 min at 298 K.[44] The hydrolysis of **13** under comparable conditions is more than an order of magnitude slower, with a half-life of 8.2 h. It is well documented that the coordination of an η^6-arene to Ru(II) increases the lability of the coordinated water in $[(\eta^6\text{-arene})Ru(OH_2)_3]^{2+}$ compared with $[Ru(OH_2)_6]^{2+}$ (by 3 orders of magnitude), and this phenomenon is ascribed to the differences in transition-state properties and the strong trans-labilizing effect of the aromatic ligand on the coordinated water.[30] The rate of aquation, however, was found to decrease by 2 orders of magnitude when two of the aquo ligands are replaced by the π-acceptor chelating ligand bipyridine (bipy), attributable to a smaller trans effect due to competition between the arene and bipy for Ru $4d^6$ electron density.[39] The presence of the π-acceptor azo ligand in **13** decreases the rate of hydrolysis compared with the ethylenediamine analogues.

Acidity of Aquated Complex 13A and 9EtG Binding. The interaction of Ru(II) arene complexes with DNA is thought to be important with respect to their observed cytotoxicity.[2,5] In aqueous solution, for example, $[(\eta^6\text{-bip})$-

(35) Lever, A. B. P.; Nelson, S. M.; Shepherd, T. M. *Inorg. Chem.* **1965**, *4*, 810−813.
(36) Cabral, J. d. O.; King, H. C. A.; Nelson, S. M.; Shepherd, T. M.; Koros, E. *J. Chem. Soc. Sect. A* **1966**, 1348−1353.
(37) Luginbühl, W.; Zbinden, P.; Pittet, P. A.; Armbruster, T.; Bürgi, H. B.; Merbach, A. E.; ludi, A. *Inorg. Chem.* **1991**, *30*, 2350−2355.
(38) Rapaport, I.; Helm, L.; Merbach, A. E.; Bernhard, P.; Ludi, A. *Inorg. Chem.* **1988**, *27*, 873−879.
(39) Dadci, L.; Elias, H.; Frey, U.; Hörnig, A.; Koelle, U.; Merbach, A. E., Paulus, H.; Schneider, J. S. *Inorg. Chem.* **1995**, *34*, 306−315.
(40) Karlen, T.; Hauser, A.; Ludi, A. *Inorg. Chem.* **1994**, *33*, 2213−2218.
(41) Freedman, D. A.; Janzen, D. E.; Mann, K. R. *Inorg. Chem.* **2001**, *40*, 6009−6016, and references therein.
(42) Sadimenko, A. P.; Basson, S. S. *Coord. Chem. Rev.* **1996**, *147*, 247−297.
(43) Sullivan, B. P.; Salmon, D. J.; Meyer, T. J.; Peedin, J. *Inorg. Chem.* **1979**, *18*, 3369−3374.
(44) Wang, F.; Chen, H.; Parsons, S.; Oswald, I. D. H.; Davidson, J. E.; Sadler, P. J. *Chem.—Eur. J.* **2003**, *9*, 5810−5820.

$Ru(en)Cl]^+$ binds specifically to guanosine[4] and this reaction proceeds through the initial aquation of the chlorido complex. The pK_a of the coordinated water of the aqua adduct $[(\eta^6\text{-bip})Ru(en)OH_2]^{2+}$ is 7.71,[44] which means that at physiological pH (close to pH 7) the complex exists mainly in the aqua form. The increased reactivity of $Ru-OH_2$ versus Ru−OH toward guanine bases has been reported previously for other Ru(II) arene complexes.[4]

In contrast, the pK_a* of the aqua adduct **13A** (4.60) is considerably lower. The high acidity of the coordinated water in **13A** is indicative of a low electron density at ruthenium since the acidity of a coordinated water molecule increases with decreasing charge density on the metal.[39] At physiological pH (ca. 7), the complex would exist predominantly in the more inert hydroxo form. Hence, it is perhaps not suprising that it has a lowered affinity for DNA bases. After 24 h, only ca. 28% of **13A** reacted with 1 mol equiv of 9EtG to form $[(\eta^6\text{-}p\text{-cym})Ru(azpzy\text{-}NMe_2)(9EtG)]^{2+}$.

Cytotoxicity. No compounds containing the phenylazopyridine ligand azpy exhibited cytotoxicity against either A2780 human ovarian or A549 human lung cancer cells. With the ligands azpy-NMe_2 and azpy-OH, complexes **8**, **10**, and **12** show cytotoxicity in both cell lines, as do complexes **13** and **16** containing the azpyz-NMe_2 ligand. There appears to be no correlation between the aqueous solution chemistry and the observed cytotoxicity. The species responsible for the cytotoxicity could be the intact cation, the corresponding aqua/hydroxo complex, or the Ru(II) phenylazopyridine complex produced after arene loss, since the speciation over 24 h suggests that all three species could be present in varying amounts.

Intact cations might exert a cytotoxic effect by mechanisms which include modification of mitochondrial membrane permeability (as observed, for example, with lipophilic cations of Au(I) carbene complexes[45]) or DNA intercalation by the arene (when extended) or the azopyridine ligand. Recently the cytotoxicity of several isomers of $[Ru(azpy)_2(bipy)]^{2+}$ incapable of hydrolysis has been reported.[12] Anticancer activity has also recently been reported for the complex $[(\eta^6\text{-hmb})Ru(en)(SPh)]^+$ (hmb = hexamethylbenzene) which does not undergo hydrolysis.[46]

Loss of the η^6-arene would create three potentially reactive sites on Ru(II) for interaction with DNA or other biomolecules. Arene loss followed by binding to a 14-mer oligonucleotide has been reported[47] for the Ru(II) arenes $[(\eta^6\text{-}p\text{-cym})Ru(pta)Cl_2]$ and $[(\eta^6\text{-}p\text{-cym})Ru(pta\text{-}Me)Cl_2]Cl$ (pta is 1,3,5-triaza-7-phosphatricyclo[3.3.1.1]decane).

The aquated phenylazopyridine complexes may bind to DNA bases by a mechanism similar to that proposed for analogous Ru(II) arene complexes.[4] However, the pK_a value of the coordinated water in azo arene complexes is predicted to be low, as the metal is more electropositive. This might give rise to a lowered affinity for DNA. While the phenylazopyrazole complex **13** undergoes hydrolysis (and no arene loss), it binds to 9EtG to a limited extent only.

All the azo complexes prepared here contain stereogenic ruthenium centers but exist as racemic mixtures. The biological activities of the enantiomers could, in principle, differ, and it would be interesting in future work to attempt to resolve them.

Conclusions

A series of intensely colored Ru(II) arene complexes containing the chelating azo ligands azpy, azpy-NMe_2, azpyz-NMe_2, and azpy-OH has been synthesized and characterized by X-ray crystallography, ^{1}H NMR, and UV−vis spectroscopy. The η^6-arene in the azopyridine complexes appears to be more labile than in Ru(II) arene complexes containing chelated ligands such as ethylenediamine, especially for complexes containing biphenyl as the arene. Arene loss is attributable to the strong π-acceptor character of phenylazopyridine ligands, which effectively compete with the arene for π-back-donation from the metal. There is evidence for this competition in the crystal structures, where Ru arene centroid distances are longer than in the corresponding en complexes, and in NMR spectra where ^{1}H NMR arene resonances are shifted to a lower field upon chelation of phenylazo pyridine, compared with the corresponding starting dimers. For the *p*-cym complexes, hydrolysis was detected for **5** (azpy-NMe_2) and **9** (azpy-OH) but not for **1** (azpy). Thus, hydrolysis is favored by an increase in the electron density on ruthenium (increase in the pK_a of the pyridine, increase in electron density on Ru), but arene loss is still competitive. Complex **13**, containing the azopyrazole ligand, hydrolyzes fully, and this can be rationalized by the inability of pyrazole compared to pyridine to act as a π-acceptor, so increasing the electron density on Ru further. This may also explain why no arene loss was detected for **13**: the arene experiences less competition for π-back-donation. Several of these compounds exhibit cytotoxicity against both A2780 and A549 cancer cell lines and may have a novel mechanism of action compared to en Ru(II) arenes.

Acknowledgment. We thank Oncosense Ltd, BBSRC (CASE studentship for S.J.D.) and Wellcome Trust (Edinburgh Protein Interaction Centre) for support, Emily Jones and Daniel Cole (Oncosense Ltd) for excellent assistance with the cytotoxicity tests, and members of EC Cost Action D20 for stimulating discussions.

Note Added After Print Publication: Due to an ACS production error, two of the electronic transitions listed on p 10888 were incorrect and two of the traces were referenced incorrectly in the caption of Figure 6 on p 10889 in the version published on the Web December 7, 2006 (ASAP) and published in the December 25, 2006 issue (Vol. 45, No. 26, pp 10882−10894); the correct electronic version of the paper was published February 16, 2007, and an Addition and Correction appears on p 1508 in the February 19, 2007 issue (Vol. 46, No. 4).

Supporting Information Available: Details of synthesis of ligands, ^{1}H NMR assignments, and Figures S1−S10. This material is available free of charge via the Internet at http://pubs.acs.org.

IC061460H

(45) Barnard, P. J.; Baker, M. V.; Berners-Price, S. J.; Day, D. D. *J. Inorg. Biol. Chem.* **2004**, *98*, 1642−1647.

(46) Wang, F.; Habtemariam, A.; van der Geer, E. P. L.; Fernandez, R.; Melchart, M.; Deeth, R. J.; Aird, R.; Guichard, S.; Fabbiani, F. P. A.; Lozano-Casal, P.; Oswald, I. D. H.; Jodrell, D. I.; Parsons, S.; Sadler, P. J. *Proc. Natl. Acad. Sci U.S.A.* **2005**, *102*, 18269−18274.

(47) Dorcier, A.; Dyson, P. J.; Gossens, C.; Rothlisberger, U.; Scopelliti, R., Tavernelli, I. *Organomet.* **2005**, *24*, 2114−2123.